JPET Fast Forward. Published on July 6, 2012 as DOI: 10.1124/jpet.112.194100

TITLE PAGE

Inhibiting Glycogen Synthase Kinase-3 Decreases 12-O-Tetradecanoylphorbol-13-Acetate-Induced Interferon-γ-Mediated Skin Inflammation

Chia-Yuan Hsieh, Chia-Ling Chen, Cheng-Chieh Tsai, Wei-Ching Huang, Po-Chun Tseng, Yee-Shin Lin, Shun-Hua Chen, Tak-Wah Wong, Pui-Ching Choi, and Chiou-Feng Lin

Institute of Clinical Medicine (C.-Y.H., C.-C.T., W.-C.H., P.-C.T., P.-C.C., C.-F.L.), Center of Infectious Disease and Signaling Research (C.-L.C., Y.-S.L., C.-F.L.), Institute of Basic Medical Sciences (C.-C.T., Y.-S.L., S.-H.C., C.-F.L.), Department of Microbiology and Immunology (Y.-S.L., S.-H.C., C.-F.L.), Department of Dermatology (T.-W.W.), and Department of Biochemistry and Molecular Biology (T.-W.W.), College of Medicine, National Cheng Kung University, Tainan, Taiwan and Department of Nursing (C.-C.T.), Chung Hwa University of Medical Technology, Tainan, Taiwan

RUNNING TITLE PAGE

Running title: GSK-3 Facilitates Skin Inflammation

Corresponding author:

Chiou-Feng Lin, PhD.

Institute of Clinical Medicine

College of Medicine

National Cheng Kung University

Tainan 701, Taiwan

886-6-2353535 ext. 4240

886-6-2758781 (fax)

Email: cflin@mail.ncku.edu.tw

Document statistics:

Text pages: 28

Tables: 0

Figures: 7

References: 40

Words in abstract: 190

Words in introduction: 605

Words in discussion: 1095

Abbreviations: GSK-3, glycogen synthase kinase-3; pGSK-3, phospho-GSK-3; pGS, phospho-glycogen synthase; IFN-γ, interferon-γ; IFNGR1, IFN-γ receptor type 1; *Ifngr1*$^{-/-}$, IFN-γ receptor 1 deficiency; T-bet, T-box transcription factor Tbx21; Jak, Janus kinase; STAT1, signal transducer and activator of transcription 1; pSTAT1, phospho-STAT1; IRF-1, interferon regulatory factor 1; Th, T helper; NK, natural killer; PBS, phosphate-based saline; DMSO, dimethyl sulfoxide; TPA, 12-O-tetradecanoylphorbol-13-acetate; BIO, 6-bromoindirubin-3'-oxime; shRNA, short hairpin RNA; shLuc, shRNA-luciferase gene; RPMI, Roswell Park Memorial Institute medium; FBS, fetal bovine serum; DAPI, 4',6-diamidino-2-phenylindole; HRP, horseradish peroxidase; H&E, hematoxylin and eosin; IHC, immunohistochemistry; IOD, integrated optical density; ns, not significant

Recommended section assignment: Inflammation, Immunopharmacology and Asthma

Abstract

Glycogen synthase kinase (GSK)-3 facilitates interferon (IFN)-γ signaling. Because IFN-γ is involved in inflammatory skin diseases, such as psoriasis, the aim of this study was to investigate the pathogenic role of GSK-3 in 12-O-tetradecanoylphorbol-13-acetate (TPA)-induced IFN-γ-mediated ear skin inflammation. TPA (3 μg per ear) induced acute skin inflammation in the ears of C57BL/6 mice including edema, infiltration of granulocytes but not T cells, and IFN-γ receptor 1-mediated deregulation of intercellular adhesion molecule 1 (CD54). TPA/IFN-γ induced GSK-3 activation, which in turn activated signal transducer and activator of transcription 1. Inhibiting GSK-3 pharmacologically, by administering 6-bromoindirubin-3'-oxime (1.5 μg per ear), and genetically, with lentiviral-based short-hairpin RNA, reduced TPA-induced acute skin inflammation but not T-cell infiltration. Notably, inhibiting GSK-3 decreased TPA-induced IFN-γ production and the nuclear translocation of T-box transcription factor Tbx21, a transcription factor of IFN-γ, in CD3-positive T cells. In chronic TPA-induced skin inflammation, inhibiting GSK-3 attenuated epidermis hyperproliferation and dermis angiogenesis. These results demonstrate the dual role of GSK-3 in TPA-induced skin inflammation that is not only to facilitate IFN-γ signaling but also to regulate IFN-γ production. Inhibiting GSK-3 may be a potential treatment strategy to prevent such effects.

JPET Fast Forward. Published on July 6, 2012 as DOI: 10.1124/jpet.112.194100
This article has not been copyedited and formatted. The final version may differ from this version.

Introduction

Skin provides the largest immunity barrier because disordered immune responses result in a large variety of inflammatory skin diseases, including psoriasis, among others (Kupper and Fuhlbrigge, 2004). The causes of psoriasis can be genetic, infectious, or environmental stimuli (Nestle et al., 2009; Cojocaru et al., 2010). Cytokines released from Th1 and Th17 cells are believed to facilitate immunopathogenesis in immune-mediated psoriasis by inducing keratinocytes to generate inflammatory antimicrobial peptides, cytokines, and chemokines (Nestle et al., 2009; Zaba et al., 2009). Recent investigations of psoriasis have focused primarily on the pathogenic role of Th17 cells (Krueger et al., 2007; Zheng et al., 2007; Steinman, 2010). However, the levels of interferon (IFN)-γ in serum are positively correlated with disease severity in psoriasis (Szegedi et al., 2003; Abdallah et al., 2009; Takahashi et al., 2010). Notably, IFN-γ-regulated gene expression is pivotal in psoriasis, and IFN-γ receptors (IFNGR) 1 and 2 are overexpressed in psoriatic peripheral blood mononuclear cells; additionally, the activation of signal transducer and activator of transcription (STAT) 1 has been identified in psoriatic skin lesions (Yao et al., 2008). These results suggest an important role for IFN-γ, a Th1 cytokine, in the progression of skin inflammation.

IFN-γ belongs to a family of type II IFN cytokines that are released from Th1, natural killer (NK), and NKT cells, and it promotes anti-microbial responses, antigen processing, inflammation, growth suppression, cell death, tumor immunity, and autoimmunity (Platanias, 2005; Schoenborn and Wilson, 2007; Saha et al., 2010). After binding to IFNGR, IFN-γ activates Janus kinase (Jak) 1 and Jak2 sequentially. Jak1 then induces STAT1 binding to IFNGR1 followed by Jak2-mediated STAT1 phosphorylation at the tyrosine residue 701 (Tyr701) (Bach *et al.*, 1997; Ramana *et al.*, 2002). The activated STAT1 translocates to the nucleus and is necessary for the transactivation of pro-inflammatory molecules, including tumor necrosis factor-α, IFN-γ-induced protein 10, monocyte chemotactic protein-1, regulated upon activation, normal T-cell expressed, and intercellular adhesion molecule 1 (CD54), but not the anti-inflammatory cytokine interleukin-10 (Donnelly et al., 1995; Schroder et al., 2004; Hu et al., 2006). IFN-γ also triggers inducible nitric oxide synthase expression to facilitate generation of nitric oxide (Lorsbach et al., 1993; Gao et al., 1997). In addition to STAT1, IFN regulatory factor 1 (IRF-1), and nuclear factor kappa-light-chain-enhancer of activated B cells are activated, which are involved in typical IFN-γ signaling and inflammation (Ramana et al., 2002; Schroder et al., 2004; Kai et al., 2010).

Furthermore, the pathogenic role of IFN-γ signaling has been demonstrated in murine psoriasis-like skin inflammation (Arakura et al., 2007; Sarra et al., 2011).

Glycogen synthase kinase (GSK)-3, a serine/threonine kinase, positively regulates multiple inflammatory diseases including sepsis, arthritis, colitis, and multiple sclerosis by influencing several critical transcription factors, such as NF-κB, nuclear factor of activated T cells, and STATs (Beurel *et al.*, 2010; Kai *et al.*, 2010; Wang *et al.*, 2011). Recent studies suggest that GSK-3 facilitates IFN-γ-mediated inflammation by mediating STAT1 activation (Tsai *et al.*, 2009). Furthermore, GSK-3 facilities the Con A-induced IFN-γ-mediated immune hepatic injury by promoting STAT1 activation and the nuclear translocation of T-box transcription factor TBX21 (Tsai *et al.*, 2011). We therefore hypothesized that GSK-3 may facilitate IFN-γ-mediated skin inflammation. The model of inflammation used in this study was cutaneous inflammation induced using 12-O-tetradecanoylphorbol -13-acetate (TPA) treatment on rodent ears. TPA-induced acute skin inflammation causes ear edema and inflammatory infiltration. Long-term treatment with TPA induces skin epidermal hyperproliferation, dermal immune cell infiltration, and angiogenesis (De Vry et al., 2005; Park et al., 2011). In this study, we investigated the role of GSK-3 in TPA-induced skin inflammation *in vivo* and the role of IFN-γ signaling in epidermal keratinocytes *in vivo* and *in vitro*.

JPET Fast Forward. Published on July 6, 2012 as DOI: 10.1124/jpet.112.194100
This article has not been copyedited and formatted. The final version may differ from this version.

Methods

Drugs and Reagents

TPA and GSK-3 inhibitor 6-bromoindirubin-3'-oxime (BIO) were purchased from Sigma-Aldrich (St. Louis, MO). Recombinant human IFN-γ was obtained from PeproTech (Rocky Hill, NJ). DAPI (4', 6-diamidino-2-phenylindole), and mouse anti-β-actin mAb were obtained from Sigma-Aldrich. Alex Fluor 488-labeled anti-mouse CD45, CD3ε, Gr-1, CD54, or CD31 and anti-mouse T-box transcription factor Tbx21 (T-bet) were obtained from BioLegend (San Diego, CA). Alexa Fluor 488- or 594-labeled and horseradish peroxidase (HRP)-conjugated goat anti-mouse, goat anti-rabbit, goat anti-rat, and donkey anti-goat IgG were from Invitrogen (Carlsbad, CA). The antibody for mouse signal transducers and activators of transcription (STAT) 1, phospho-glycogen synthase (GS, S641), and glycogen synthase kinase (GSK)-3β were obtained from Cell Signaling Technology (Beverly, MA). Anti-mouse phospho-STAT1 (Y701), phospho-GSK-3α/β (Y279/Y216), and Ki-67 antibodies were obtained from Abcam (Cambridge, MA). Anti-GSK-3α/β was obtained from Santa Cruz (Santa Cruz, CA). Rat mAb targeted against mouse IFN-γ was obtained from Bender MedSystems (Burlingame, CA). Anti-mouse Gr-1 neutralizing Ab (clone RB6-8C5) was obtained from eBioscience (San Diego, CA).

Animal Treatment

The eight- to twelve-week-old progeny of wild type C57BL/6 mice and IFNGR1-deficient (*Ifngr1*$^{-/-}$) mice on a C57BL/6 background were purchased from the Jackson Laboratory (Bar Harbor, ME). They were fed standard laboratory chow and water ad libitum in the Laboratory Animal Center of the National Cheng Kung University. The animals were raised and cared for according to the guidelines set by the National Science Council, Taiwan. The experimental protocols adhered to the rules of the Animal Protection Act of Taiwan and were approved by the Laboratory Animal Care and Use Committee of National Cheng Kung University (IACUC Approval No: 99127). As shown previously, to establish the TPA-induced acute skin inflammatory model, 30 μl of phosphate-buffered saline (PBS, pH 7.4), dimethyl sulfoxide (DMSO) diluted in PBS as a solvent control, and 50 μg ml^{-1} TPA (Sigma-Aldrich, St. Louis, MO) dissolved in solvent control (3 μg per ear) with or without the optimal dosage of 25 μg ml^{-1} of the GSK-3 inhibitor BIO (Sigma-Aldrich) (Tsai *et al.*, 2011) dissolved in solvent control (1.5 μg per ear) were dropped into 1 cm^2 pieces of 100% spunlace rayon that was 0.5 mm thick, and two pieces of rayon were then placed against the inner and outer surface of each

ear for 1 h as one treatment. This chronic skin-inflammation model is modified from that developed by De Vry *et al.* (De Vry et al., 2005; Park et al., 2011). For chronic TPA-induced cutaneous inflammation, we spaced the treatment our over 3 days and repeated the treatment six times over 15 days. On day 16, the mice were administered a lethal overdose of intraperitoneal pentobarbital (200 mg kg^{-1}), and their ear tissue was harvested at the indicated times post-injection.

Cell Culture and Cytotoxicity Assay

Human keratinocyte HaCaT cells were provided by Chia-Yu Chi, Division of Clinical Research, National Health Research Institutes, Taiwan. The cells were routinely grown on plastic in RPMI1640 (Invitrogen Life Technologies, Rockville, MD) containing 10% heat-inactivated fetal bovine serum (FBS; Invitrogen Life Technologies), 50 U penicillin, and 50 μg ml^{-1} streptomycin and were maintained in a humidified atmosphere containing 5% CO_2.

Immunohistochemistry and Immunostaining

All tissue sections were deparaffinized, rehydrated, incubated with 3% H_2O_2 in methanol for 15 min, and subjected to heat-induced antigen retrieval by autoclaving them for 5 min in 10 mM citric acid buffer (pH 6.0). Following 2 washes in PBS, the tissue sections and cells were mixed with primary antibodies in antibody diluents (DAKO Corporation, Carpinteria, CA, USA) and incubated at 4°C overnight. The following day, the samples were washed with PBS and then incubated with or without HRP- and Alexa Fluor 488- or 594-labeled secondary antibodies at room temperature for 1 h. For immunohistochemistry, sections were washed with PBS, developed using AEC substrate (DAKO Corporation), counterstained with hematoxylin (Sigma-Aldrich), and visualized using an inverted microscope (IX71; Olympus, Tokyo, Japan). For immunostaining, sections and cells were washed with PBS and visualized using a DP70 camera and a fluorescent right BX51 microscope (Olympus, Tokyo, Japan) or a linear sequential C1Si laser scanning head and an Eclipse TE2000-E inverted microscope (Nikon Corp., Tokyo, Japan). DAPI (1:200; Sigma-Aldrich) was added for nuclear counter-staining and was applied at room temperature for 10 min. The confocal images were captured in a single x-y scan (100× enlarged) or in 3D (150× enlarged; 0.5 μm per z step). Photo-bleaching and crosstalk were excluded using a line-lambda scanning mode and sequencing laser excitation at 543, 488, and 405 nm. The confocal images were generated using EZ-C1 software (NIKON Corp., Tokyo, Japan).

JPET Fast Forward. Published on July 6, 2012 as DOI: 10.1124/jpet.112.194100
This article has not been copyedited and formatted. The final version may differ from this version.

H&E Staining

For histopathological observations, portions of the ear tissue were fixed in 10% neutral-buffered formalin solution and then dehydrated in graded alcohol solutions. The fixed tissue was embedded in paraffin and sliced into 4-μm-thick sections. The tissue sections were mounted on regular glass slides, deparaffinized in xylene, rehydrated in decreasing concentrations of ethanol, and stained with hematoxylin and eosin (H&E).

Images Quantification Analysis

To evaluate the pathological parameters including ear thickness, number of infiltrating cells, protein expression, and phosphorylation levels, pictures were quantified using three low-power fields (10× or 20× objective) of each ear section (n = 3 per group) using Image-Pro Plus version 6.0 software (Media Cybernetics, Inc., Bethesda, MD). The object analyzed in each image was calibrated and quantified as described below. For ear thickness and epidermis thickness, we measured the average ear thickness in each low-power field directly. For number of infiltrating cells in each tissue, we first determined the optical RGB intensity range using fields from tissue from the TPA group and then established the appropriate standard RGB intensity range for each image of each cell marker. We then used the appropriate standard RGB intensity range for each cell marker to count the numbers of cells staining positively for CD45, CD3, Gr-1, CD54, IFN-γ, CD31, and Ki-67. For quantifying the level of phospho-GSK-3β Tyr216 (pGSK-3) and phospho-GS Ser641 (pGS), we used the same protocol to establish the standard RGB intensity range and then used the integrated optical density (IOD) as the level of pGSK-3 and pGS. The pGSK-3 IOD of each group divided by the average IOD of pGSK-3 of the PBS control group was used to calculate the activated GSK-3 index. We used the AOI (area of interest) mode to separate the epidermal- or dermal-expressed signal within each field.

Short Hairpin RNA *In Vitro* and *In Vivo*

All shRNA clones were obtained from the National RNAi Core Facility (Institute of Molecular Biology/Genomic Research Center, Academia Sinica, Taipei, Taiwan). Lentiviruses were prepared and cells were infected according to previously described protocols (Tsai *et al.*, 2009). Briefly, GSK-3 protein levels in HaCaT cells, human keratinocyte cells, were down-regulated using lentiviral-mediated expression of a short hairpin RNA (shRNA) that targeted human GSK-3α (TRCN0000221526, containing the shRNA target sequence

JPET Fast Forward. Published on July 6, 2012 as DOI: 10.1124/jpet.112.194100
This article has not been copyedited and formatted. The final version may differ from this version.

5'-CTACATCTGTTCTCGCTACTA-3') and human GSK-3β (TRCN0000040001, containing the target sequence 5'-GCTGAGCTGTTACTAGGACAA-3'). HaCaT cells were transduced with the lentivirus using the appropriate multiplicity of infection in complete growth medium supplemented with 8 μg ml^{-1} polybrene (Sigma-Aldrich). After transduction for 24 h and puromycin (Calbiochem, San Diego, CA) selection for 3 days, protein expression was analyzed using Western blotting. For *in vivo* knockdown, the lentivirus containing shRNA targeting mouse GSK-3β (TRCN0000012615, containing the target sequence 5'-CATGAAAGTTAGCAGAGATAA-3') was pre-incubated for 5 min on ice with 8 μg ml^{-1} polybrene and then added to 60 μl of lentiviral solution (including 1.2×10^6 p.f.u.) in a 1-cm^2 piece of 0.5-mm-thick 100% spunlace rayon. Two pieces of rayon were then placed against the inner and outer surface of the ear for 24 h before TPA treatment.

Western Blotting

Harvested cells were lysed using a buffer containing 1% Triton X-100, 50 mM Tris (pH 7.5), 10 mM EDTA, 0.02% NaN_3, and a protease inhibitor cocktail (Roche Boehringer Mannheim Diagnostics, Mannheim, Germany). Following one freeze-thaw cycle, the cell lysates were centrifuged at 12,000 rpm at 4°C for 20 min. Lysates were boiled in sample buffer for 5 min. Proteins were then subjected to SDS-PAGE and transferred to PVDF membranes (Millipore, Billerica, MA, USA) using a semi-dry electroblotting system. After blocking with 5% skim milk in PBS, membranes were incubated with a 1/1000 dilution of primary antibodies at 4°C overnight. Membranes were then washed using 0.05% PBS-Tween 20 and incubated with a 1/5000 dilution of horseradish peroxidase-conjugated secondary antibodies at room temperature for 1 h. After washing, membranes were soaked in an ECL solution (PerkinElmer Life Sciences Inc., Boston, MA, USA) for 1 min and then exposed to film (BioMax; Eastman Kodak, Rochester, NY, USA).

Luciferase Reporter Assay

For the luciferase reporter assay, the cells were transiently co-transfected using a GeneJammer reagent (Stratagene) with an IRF1 promoter-driven luciferase reporter (0.2 μg) and 0.01 μg of Renilla luciferase-expressing plasmid (pRL-TK; Promega). Twenty-four hours after the transfection, the cells were treated with IFN-γ for 3 h, lysed, and then harvested for luciferase and Renilla measurement using a luciferase assay kit (Dual-Glo; Promega). For each lysate, the firefly luciferase activity was normalized to the Renilla luciferase activity to assess transfection efficiency.

Granulocyte Depletion

For the depletion of granulocytes, each mouse received intraperitoneal injections of 50 μg of monoclonal rat-anti-mouse Gr-1 antibody (clone RB6-8C5; eBioscience, San Diego, CA) in 100 μl PBS (Jablonska *et al.*, 2010).

Statistical Analysis

Values are expressed as the mean ± S.D. The groups were compared using Student's two-tailed unpaired *t*-tests or using a one-way ANOVAs in GraphPad Prism version 5. A value of $p < 0.05$ was considered to be statistically significant.

JPET Fast Forward. Published on July 6, 2012 as DOI: 10.1124/jpet.112.194100
This article has not been copyedited and formatted. The final version may differ from this version.

Results

IFNGR1 Is Required for TPA-Induced Acute Skin Inflammation

IFN-γ is associated with immunopathogenesis in psoriasis (Nestle et al., 2009; Takahashi et al., 2010). Using TPA (3 μg per ear)-induced acute skin inflammation in C57BL/6 mice, as shown previously (Park et al., 2011), we found that TPA induced STAT1 activation, which was detected using STAT1 phosphorylation at Tyr701 and protein expression in the epidermis and dermis of wild type but not IFNGR1-deficient (*Ifngr1*$^{-/-}$) mice (n = 3 per group, Fig. 1A). H&E staining (Fig. 1B) showed that ear thickness was significantly (215.9 ± 48.8, DMSO, only vs. 503.2 ± 142.5, TPA, $p < 0.001$) increased in TPA-treated wild type mice but was significantly (503.2 ± 142.5, wild type, vs. 382.5 ± 59.5, *Ifngr1*$^{-/-}$, $p < 0.05$) attenuated in *Ifngr1*$^{-/-}$ mice compared with the DMSO-treated group (Fig. 1C). Furthermore, IFNGR1 deficiency significantly attenuated the TPA-induced infiltration of leukocytes (367.1 ± 204.8, wild type, vs. 165.1 ± 28.8, *Ifngr1*$^{-/-}$, $p < 0.05$, Fig. 1D) and granulocytes (238.2 ± 156.5, wild type, vs. 76.3 ± 49.8, *Ifngr1*$^{-/-}$, $P < 0.01$, Fig. 1F) and the expression of adhesion molecule CD54 (206.9 ± 78.6, wild type, vs. 125.1 ± 72.9, *Ifngr1*$^{-/-}$, $p < 0.05$, Fig. 1G) but not the infiltration of CD3^{+} T cells (Fig. 1E). These results indicate that IFN-γ signaling is essential for TPA-induced acute skin inflammation including edema, granulocyte infiltration, and CD54 expression but not T cell infiltration.

TPA Activates GSK-3 and Induces GSK-3-Regulated IFN-γ Signaling

We previously demonstrated that GSK-3 facilitates IFN-γ-STAT1 signaling (Tsai *et al.*, 2009). We therefore hypothesized that GSK-3 facilitates TPA-induced acute skin inflammation. AEC-based immunohistochemistry (Fig. 2A) showed that TPA-induced GSK-3 activation (1.0 ± 0.4, DMSO only, vs. 3.1 ± 1.9, TPA, $p < 0.05$, Fig. 2B), which was detected as GSK-3β phosphorylation at Tyr216, an active residue of GSK-3β, and glycogen synthase phosphorylation at Ser641, a substrate of GSK-3, as shown previously (Tsai *et al.*, 2011), in the epidermis (1.4 ± 0.5, DMSO only, vs. 6.5 ± 3.1, TPA, $p < 0.05$, Fig. 2C) and dermis (0.9 ± 0.4, DMSO only, vs. 4.2 ± 2.8, TPA, $p < 0.05$, Fig. 2D). To verify the role of activated GSK-3, GSK-3 was inhibited using the inhibitor BIO, which binds within the ATP-binding pocket of GSK-3. The results showed that treatment with BIO (1.5 μg per ear, the maximum dosage selected from three dilutions; data not shown), reduced TPA-induced STAT1 activation and expression in the epidermis but not the dermal infiltrate of wild type mice (Fig. 2E). We next

JPET Fast Forward. Published on July 6, 2012 as DOI: 10.1124/jpet.112.194100
This article has not been copyedited and formatted. The final version may differ from this version.

investigated the role of GSK-3 in epidermal keratinocytes in response to IFN-γ. The expression of GSK-3α/β was knocked down in HaCaT human keratinocytes using a lentiviral-based shRNA approach (Fig. 2F). A luciferase reporter assay for IRF1 promoter transactivation showed that the knockdown of GSK-3α/β, consistent with BIO (2.5 μM) treatment, significantly (11.6 ± 5.2, DMSO only, vs. 5.2 ± 2.8, BIO, 5.5 ± 1.8, shGSK-3α, and 4.2 ± 1.3, shGSK-3β, $p < 0.05$) inhibited IFN-γ (10 ng ml^{-1}) signaling (Fig. 2G). These results demonstrate that TPA induces GSK-3 activation in the epidermis and leads to GSK-3 regulation of IFN-γ signaling.

GSK-3 Facilitates TPA-Induced Acute Skin Inflammatory Responses

BIO was next used to investigate whether inhibiting GSK-3 reduces TPA-induced acute skin inflammatory responses. Notably, inhibiting GSK-3 attenuated TPA-induced ear swelling (Fig. 3A and Supplemental Figure 1A). Furthermore, ears treated with BIO displayed an attenuation of the TPA-induced increased ear thickness (501.0 ± 138.9, TPA only, vs. 299.0 ± 41.0, TPA + BIO, $p < 0.05$, Fig. 3B), the infiltration of leukocytes (511.7 ± 203.1, TPA only, vs. 125.5 ± 84.7, TPA + BIO, $p < 0.01$, Fig. 3C) and granulocytes (238.2 ± 156.5, TPA only, vs. 102.5 ± 77.1, TPA + BIO, $p < 0.01$, Fig. 3E), and the expression of CD54 (240.1 ± 94.1, TPA only, vs. 140.6 ± 93.5, TPA + BIO, $p < 0.01$, Fig. 3F) but not $CD3^+$ T cell infiltration (Fig. 3D). Thus, TPA induces the infiltration of granulocytes. The depletion of granulocytes, using an anti-Gr-1 antibody, suggests that granulocytes may be pathogenic in TPA-induced acute ear edema (Supplemental Figures 1B and C). These results demonstrate that GSK-3 activation is pathogenic for TPA-induced acute skin inflammation including edema, granulocyte infiltration, and CD54 expression but not T cell infiltration.

Epidermal GSK-3 Facilitates TPA-Induced Edema and Granulocyte Infiltration

To further clarify the role of GSK-3 in epidermal keratinocytes *in vivo*, we created a local knockdown of GSK-3β using lentiviral-based shRNA interference in the ears of C57BL/6 mice. Our GSK-3β immunohistochemical results (Fig. 4A) show that GSK-3β knockdown reduces GSK-3β expression in the epidermis markedly (4.9 ± 1.5, shLuc, vs. 2.6 ± 0.9, shGSK-3β, $p < 0.01$, Fig. 4B). Analysis of histological morphology (Fig. 4C) revealed that the epidermal knockdown of GSK-3β significantly attenuated both TPA-induced ear edema (515.3 ± 73.6, shLuc, vs. 416.6 ± 39.9, shGSK-3β, $p < 0.05$, Fig. 4D) and granulocyte infiltration (272.6 ± 88.6, shLuc, vs. 169.3 ± 61.0, shGSK-3β, $p < 0.01$, Fig. 4E). These results imply that GSK-3 activation is key for TPA-induced edema and granulocyte infiltration.

JPET Fast Forward. Published on July 6, 2012 as DOI: 10.1124/jpet.112.194100
This article has not been copyedited and formatted. The final version may differ from this version.

GSK-3 Facilitates TPA-Induced IFN-γ Production in CD3-Positive T Cells by Regulating T-bet Nuclear Translocation

The pathogenesis of immune-mediated psoriasis is thought to be T cell-mediated (Schon and Boehncke, 2005). Our findings show that GSK-3-regulated IFN-γ signaling is not involved in CD3-positive T cell infiltration. Immunohistochemistry for IFN-γ (Fig. 5A) showed that TPA markedly induced IFN-γ production at 4 h (13.3 ± 7.8, DMSO only, vs. 37.1 ± 10.1, TPA, $p < 0.001$, Fig. 5B) compared with the DMSO-treated group. However, treatment with BIO significantly (37.1 ± 10.1, TPA only, vs. 20.6 ± 7.2, TPA + BIO, $p < 0.05$) decreased TPA-induced dermal IFN-γ expression. GSK-3 is required for the nuclear translocation of T-bet (Hwang *et al.*, 2005; Tsai *et al.*, 2011). Immunostaining and confocal image analysis identified TPA-induced GSK-3 activation, which was determined by the phosphorylation of GSK-3 at Tyr216 in CD3 positive T cells (Fig. 5C). Notably, inhibiting GSK-3 decreased the TPA-induced T-bet nuclear translocation in CD3-positive T cells (Fig. 5D and Supplemental Figure 2). These results demonstrate that GSK-3 activation in T cells facilitates IFN-γ production by facilitating T-bet nuclear translocation in TPA-induced acute skin inflammation.

GSK-3 Facilitates IFN-γ-Mediated Chronic TPA-Induced Psoriasis-Like Cutaneous Inflammation

To further clarify the role of GSK-3 in skin inflammation, we also assessed the protective effects of GSK-3 inhibition in a model of chronic TPA treatment (Fig. 6A). BIO treatment strikingly attenuated TPA-induced edema and epidermal swelling (Fig. 6B), ear thickness (539.1 ± 119.7, TPA only, vs. 327.7 ± 51.1, TPA + BIO, $p < 0.01$, Fig. 6C), and epidermal thickness (73.6 ± 15.1, TPA only, vs. 38.7 ± 4.6, TPA + BIO, $p < 0.01$, Fig. 6D). To investigate the role of GSK-3 in IFN-γ-regulated chronic TPA-induced cutaneous inflammation, immunostaining of Ki-67, a proliferation marker, and CD31, an endothelial cell marker, were used (Supplemental Figure 3). The results showed that inhibiting GSK-3 significantly suppressed TPA-induced epidermal cell proliferation (206.8 ± 66.3, TPA only, vs. 90.7 ± 44.2, TPA + BIO, $p < 0.05$, Fig. 6E) and dermal angiogenesis (89.0 ± 28.1, TPA only, vs. 25.0 ± 12.5, TPA + BIO, $p < 0.01$, Fig. 6F). Immunostaining showed that chronic TPA treatment also induced GSK-3 activation (Fig. 6G). These results demonstrate that inhibiting GSK-3 attenuates chronic TPA-induced cutaneous inflammation including edema, epidermal proliferation, and angiogenesis.

JPET Fast Forward. Published on July 6, 2012 as DOI: 10.1124/jpet.112.194100
This article has not been copyedited and formatted. The final version may differ from this version.

Discussion

In this study, we used a murine model of TPA-induced skin inflammation to demonstrate that the activation of GSK-3 not only facilitates IFN-γ signaling in keratinocytes *in vivo* and *in vitro* but is also required for IFN-γ production in T cells by activating T-bet, which is an important transcription factor for IFN-γ. Furthermore, inhibiting GSK-3 provides partial cellular protection from TPA-induced acute edema, granulocyte infiltration, and CD54 expression and TPA-induced chronic epidermal proliferation and dermal angiogenesis. These findings are summarized briefly in Fig. 7. Following cell injury-related release of damage-associated molecules, TPA induces an inflammatory response in the skin by becoming a hapten. However, the mechanism underlying activation of GSK-3 by TPA in T cells remains unclear. Our results suggest that IFN-γ can activate GSK-3 in keratinocytes *in vivo* and *in vitro*, which is consistent with our previous studies (Tsai *et al.*, 2009).

Pathological changes in the inflammatory lesions are characterized by a thickening of the epidermis, parakeratosis, elongated rete ridges, and infiltration of several cell types, including T cells, dendritic cells, neutrophils, and other immune cells (Schon and Boehncke, 2005; Nestle et al., 2009). Consistent with previous studies (De Vry et al., 2005; Park et al., 2011), this study also showed that TPA treatment induces ear edema, the infiltration of multiple types of immune cells (likely T cells and granulocytes), epidermal keratinocyte proliferation, and angiogenesis. We speculate that TPA-induced skin inflammation may act as a suitable model for investigating the important role of IFN-γ and GSK-3 in inflammation.

TPA-induced T cell infiltration remains unaffected by the absence of IFNGR1, which indicates an upstream role for T cells in IFN-γ-regulated TPA-induced skin inflammation. These results support the theory of T cell-mediated immunopathogenesis in cutaneous inflammation. Cytokines derived from activated T cells, which include Th1 and Th17, are well-known to underlie the immunopathogenesis of skin diseases. Cytokines of both Th1, such as TNF-α and IFN-γ, and Th17 cells, such as IL-17A, IL-17F, and IL-22, are thought to be the inflammatory mediators of keratinocyte activation and proliferation and for granulocyte infiltration in skin inflammation (Nestle *et al.*, 2009). We further demonstrate that depletion of granulocytes causes a decrease in TPA-induced acute ear edema. We speculate that T cell activation and granulocyte infiltration facilitates TPA-induced skin inflammation.

IFN-γ is an important pro-inflammatory cytokine for several types of psoriasis (Szegedi et al., 2003; Yao et al., 2008; Abdallah et al., 2009; Takahashi et al., 2010). To the best of our knowledge, this study provides the first evidence showing that IFNGR1 is required for

TPA-induced skin inflammation. We speculate that these findings may explain the effects of aberrant IFN-γ production (Szegedi et al., 2003; Abdallah et al., 2009; Takahashi et al., 2010) and STAT1 activation in psoriatic lesions (Yao *et al.*, 2008). Notably, inhibiting GSK-3 with BIO or lentiviral-based GSK-3β-targeted shRNA resulted in an inhibition of the TPA-induced skin inflammation. Mechanistically, GSK-3 not only facilitates IFN-γ signaling in keratinocytes but is also required for TPA-induced IFN-γ production independent of the interference with T cell infiltration. These findings are consistent with recent studies that suggest that GSK-3 facilitates IFN-γ-mediated inflammation by activating STAT1 (Tsai *et al.*, 2009). Additionally, GSK-3 facilities Con A- (Tsai *et al.*, 2011) and TPA-induced IFN-γ-mediated inflammatory activation by promoting STAT1 activation and the nuclear translocation of T-bet, which results in an increase in IFN-γ production. In addition to IFN-γ, the role of Th17 cell activation and differentiation in GSK-3 activation requires further investigation (Beurel *et al.*, 2011). The role of Th17 responses in TPA-induced skin inflammation also requires further investigation. In addition to Th1-IFN-γ-mediated skin inflammation, we speculate that inhibiting GSK-3 may also reduce Th17 responses.

Treatment with TPA induces GSK-3β activation in epidermal keratinocytes and infiltrated T cells. A limitation of this study is that is remains unclear whether TPA induces GSK-3 activation directly or indirectly through other mechanisms, such as damage-associated molecules. Previous studies suggest that the activation of GSK-3 by IFN-γ, IL-6, and GM-CSF facilitates the activation of STAT1, 3, 5, and 6 (Tsai *et al.*, 2009; Wang *et al.*, 2011). It is therefore hypothesized that these cytokines determine TPA-mediated GSK-3 activation and could induce IFN-γ, IL-6, and GM-CSF expression (Oberg *et al.*, 2001). Consistent with our previous studies (Lin et al., 2008; Tsai et al., 2009; Kai et al., 2010) and those of others (Beurel *et al.*, 2010; Wang *et al.*, 2011), treatment with IFN-γ causes GSK-3 activation followed by GSK-3-mediated STAT1 activation. We further verified that the molecular mechanism underlying IFN-γ-activated GSK-3 is the triggering of bioactive sphingolipid ceramide-mediated pathways (Tsai *et al.*, 2009; Wang *et al.*, 2011). We therefore hypothesize that the activation of GSK-3 by ceramide may be involved in TPA-activation of T cells and IFN-γ-activated keratinocytes. The involvement of ceramide signaling in TPA-induced skin inflammation requires further investigation. In addition to GSK-3β, knockdown of GSK-3α, which is a functionally redundant GSK-3 under some conditions (Beurel *et al.*, 2010; Wang *et al.*, 2011), also reduced IFN-γ signaling. Essentially, the pharmacological inhibition of GSK-3 by BIO did not exclude the involvement of GSK-3α, and it is possible that GSK-3α

activation plays a role in TPA-induced skin inflammation.

Lithium, a non-selective inhibitor of GSK-3 that competes with magnesium ions, is commonly used for treatment of bipolar disorders. Long-term oral lithium salts are associated with a variety of pharmacological side effects including gastrointestinal pain, discomfort, diarrhea, tremor, polyuria, nocturnal urination, weight gain, edema, nephrogenic diabetes insipidus, hypothyroidism, hyperparathyroidism, hypercalcemia, and lithium-induced psoriasis (Grandjean and Aubry, 2009). However, the immunopathogenesis of lithium-induced psoriasis may be different from that of typical psoriasis (Knijff *et al.*, 2005). A reduction in intracellular calcium release following lithium treatment is hypothesized as the possible mechanism underlying lithium-aggravated psoriasis (Fry and Baker, 2007). A recent study found that inhibiting GSK-3 provoked keratinocyte proliferation (Hampton *et al.*, 2011); however, there are no reports showing that GSK-3 is inhibited in psoriatic lesions or that inactive GSK-3 exacerbates psoriasis. Manipulating GSK-3 for psoriatic therapy requires further consideration, particularly with regard to the time period and dose of inhibitor treatment.

In conclusion, our study demonstrates that the inhibition of GSK-3 not only blocks IFN-γ production but also reduces IFN-γ-mediated STAT1 activation and inflammatory responses. Our results suggest that inhibiting GSK-3 using pharmacological or genetic manipulations is a potential therapeutic strategy for IFN-γ-mediated skin inflammation not only via the inhibition of IFN-γ production but also the blockade of IFN-γ signaling, granulocyte infiltration, CD54 expression, edema, epidermal hyperplasia, and angiogenesis. The findings of this study may provide insight for future pre-clinical or clinical studies that use more comparable models of IFN-γ- and GSK-3-mediated human skin diseases.

Acknowledgments

We thank the Immunobiology Core, the Research Center of Clinical Medicine, and the National Cheng Kung University Hospital, for providing services that included training, technical support, and assistance with experimental design and data analysis. We thank Huey-Kang Sytwu, M.D., Ph.D., of the Graduate Institute of Life Science, at the National Defense Medical Center, Taiwan, for assistance with lentiviral-based shRNA experiments. For image quantification, we gratefully thank Lin Trading Co., Ltd. (Taipei, Taiwan) for support regarding the Image-Pro Plus software and quantification methods.

Authorship Contributions

Participated in research design: C.-Y. Hsieh, C.-L. Chen, Y.-S. Lin, S.-H. Chen, T.-W. Wong, and C.-F. Lin.

Conducted experiments: C.-Y. Hsieh, C.-C. Tsai, W.-C. Huang, P.-C. Tseng, P.-C. Choi.

Performed data analysis: C.-Y. Hsieh, Y.-S. Lin, T.-W. Wong, and C.-F. Lin.

Wrote or contributed to the writing of the manuscript: C.-Y. Hsieh, C.-L. Chen, and Ch.-F. Lin.

References

Abdallah MA, Abdel-Hamid MF, Kotb AM and Mabrouk EA (2009) Serum interferon-gamma is a psoriasis severity and prognostic marker. *Cutis* **84**:163-168.

Arakura F, Hida S, Ichikawa E, Yajima C, Nakajima S, Saida T and Taki S (2007) Genetic control directed toward spontaneous IFN-alpha/IFN-beta responses and downstream IFN-gamma expression influences the pathogenesis of a murine psoriasis-like skin disease. *J Immunol* **179**:3249-3257.

Bach EA, Aguet M and Schreiber RD (1997) The IFN gamma receptor: a paradigm for cytokine receptor signaling. *Annu Rev Immunol* **15**:563-591.

Beurel E, Michalek SM and Jope RS (2010) Innate and adaptive immune responses regulated by glycogen synthase kinase-3 (GSK3). *Trends Immunol* **31**:24-31.

Beurel E, Yeh WI, Michalek SM, Harrington LE and Jope RS (2011) Glycogen synthase kinase-3 is an early determinant in the differentiation of pathogenic Th17 cells. *J Immunol* **186**:1391-1398.

Cojocaru M, Cojocaru IM and Silosi I (2010) Multiple autoimmune syndrome. *Maedica (Buchar)* **5**:132-134.

De Vry CG, Valdez M, Lazarov M, Muhr E, Buelow R, Fong T and Iyer S (2005) Topical application of a novel immunomodulatory peptide, RDP58, reduces skin inflammation in the phorbol ester-induced dermatitis model. *J Invest Dermatol* **125**:473-481.

Donnelly RP, Freeman SL and Hayes MP (1995) Inhibition of IL-10 expression by IFN-gamma up-regulates transcription of TNF-alpha in human monocytes. *J Immunol* **155**:1420-1427.

Fry L and Baker BS (2007) Triggering psoriasis: the role of infections and medications. *Clin Dermatol* **25**:606-615.

Gao J, Morrison DC, Parmely TJ, Russell SW and Murphy WJ (1997) An interferon-gamma-activated site (GAS) is necessary for full expression of the mouse iNOS gene in response to interferon-gamma and lipopolysaccharide. *J Biol Chem* **272**:1226-1230.

Grandjean EM and Aubry JM (2009) Lithium: updated human knowledge using an evidence-based approach: part III: clinical safety. *CNS Drugs* **23**:397-418.

Hampton PJ, Jans R, Flockhart RJ, Parker G and Reynolds NJ (2011) Lithium regulates keratinocyte proliferation via glycogen synthase kinase 3 and NFAT2 (nuclear factor of activated T cells 2). *J Cell Physiol*.

Hu X, Paik PK, Chen J, Yarilina A, Kockeritz L, Lu TT, Woodgett JR and Ivashkiv LB (2006) IFN-gamma suppresses IL-10 production and synergizes with TLR2 by regulating GSK3 and CREB/AP-1 proteins. *Immunity* **24**:563-574.

Hwang ES, Hong JH and Glimcher LH (2005) IL-2 production in developing Th1 cells is regulated by heterodimerization of RelA and T-bet and requires T-bet serine residue 508.

J Exp Med **202**:1289-1300.

Jablonska J, Leschner S, Westphal K, Lienenklaus S and Weiss S (2010) Neutrophils responsive to endogenous IFN-beta regulate tumor angiogenesis and growth in a mouse tumor model. *J Clin Invest* **120**:1151-1164.

Kai JI, Huang WC, Tsai CC, Chang WT, Chen CL and Lin CF (2010) Glycogen synthase kinase-3beta indirectly facilitates interferon-gamma-induced nuclear factor-kappaB activation and nitric oxide biosynthesis. *J Cell Biochem* **111**:1522-1530.

Knijff EM, Kupka RW, Ruwhof C, Breunis MN, Prens EP, Nolen WA and Drexhage HA (2005) Evidence that the immunopathogenic mechanism of lithium-induced psoriasis differs from that of regular psoriasis. *Bipolar Disord* **7**:388-389.

Krueger GG, Langley RG, Leonardi C, Yeilding N, Guzzo C, Wang Y, Dooley LT and Lebwohl M (2007) A human interleukin-12/23 monoclonal antibody for the treatment of psoriasis. *N Engl J Med* **356**:580-592.

Kupper TS and Fuhlbrigge RC (2004) Immune surveillance in the skin: mechanisms and clinical consequences. *Nat Rev Immunol* **4**:211-222.

Lin CF, Tsai CC, Huang WC, Wang CY, Tseng HC, Wang Y, Kai JI, Wang SW and Cheng YL (2008) IFN-gamma synergizes with LPS to induce nitric oxide biosynthesis through glycogen synthase kinase-3-inhibited IL-10. *J Cell Biochem* **105**:746-755.

Lorsbach RB, Murphy WJ, Lowenstein CJ, Snyder SH and Russell SW (1993) Expression of

the nitric oxide synthase gene in mouse macrophages activated for tumor cell killing. Molecular basis for the synergy between interferon-gamma and lipopolysaccharide. *J Biol Chem* **268**:1908-1913.

Nestle FO, Kaplan DH and Barker J (2009) Psoriasis. *N Engl J Med* **361**:496-509.

Oberg F, Wu S, Bahram F, Nilsson K and Larsson LG (2001) Cytokine-induced restoration of differentiation and cell cycle arrest in v-Myc transformed U-937 monoblasts correlates with reduced Myc activity. *Leukemia* **15**:217-227.

Park SY, Gupta D, Hurwich R, Kim CH and Dziarski R (2011) Peptidoglycan recognition protein Pglyrp2 protects mice from psoriasis-like skin inflammation by promoting regulatory T cells and limiting Th17 responses. *J Immunol* **187**:5813-5823.

Platanias LC (2005) Mechanisms of type-I- and type-II-interferon-mediated signalling. *Nat Rev Immunol* **5**:375-386.

Ramana CV, Gil MP, Schreiber RD and Stark GR (2002) Stat1-dependent and -independent pathways in IFN-gamma-dependent signaling. *Trends Immunol* **23**:96-101.

Saha B, Jyothi Prasanna S, Chandrasekar B and Nandi D (2010) Gene modulation and immunoregulatory roles of interferon gamma. *Cytokine* **50**:1-14.

Sarra M, Caruso R, Cupi ML, Monteleone I, Stolfi C, Campione E, Diluvio L, Mazzotta A, Botti E, Chimenti S, Costanzo A, MacDonald TT, Pallone F and Monteleone G (2011) IL-21 promotes skin recruitment of CD4(+) cells and drives IFN-gamma-dependent

epidermal hyperplasia. *J Immunol* **186**:5435-5442.

Schoenborn JR and Wilson CB (2007) Regulation of interferon-gamma during innate and adaptive immune responses. *Adv Immunol* **96**:41-101.

Schon MP and Boehncke WH (2005) Psoriasis. *N Engl J Med* **352**:1899-1912.

Schroder K, Hertzog PJ, Ravasi T and Hume DA (2004) Interferon-gamma: an overview of signals, mechanisms and functions. *J Leukoc Biol* **75**:163-189.

Steinman L (2010) Mixed results with modulation of TH-17 cells in human autoimmune diseases. *Nat Immunol* **11**:41-44.

Szegedi A, Aleksza M, Gonda A, Irinyi B, Sipka S, Hunyadi J and Antal-Szalmas P (2003) Elevated rate of Thelper1 (T(H)1) lymphocytes and serum IFN-gamma levels in psoriatic patients. *Immunol Lett* **86**:277-280.

Takahashi H, Tsuji H, Hashimoto Y, Ishida-Yamamoto A and Iizuka H (2010) Serum cytokines and growth factor levels in Japanese patients with psoriasis. *Clin Exp Dermatol* **35**:645-649.

Tsai CC, Huang WC, Chen CL, Hsieh CY, Lin YS, Chen SH, Yang KC and Lin CF (2011) Glycogen synthase kinase-3 facilitates con a-induced IFN-gamma-- mediated immune hepatic injury. *J Immunol* **187**:3867-3877.

Tsai CC, Kai JI, Huang WC, Wang CY, Wang Y, Chen CL, Fang YT, Lin YS, Anderson R, Chen SH, Tsao CW and Lin CF (2009) Glycogen synthase kinase-3beta facilitates

IFN-gamma-induced STAT1 activation by regulating Src homology-2 domain-containing phosphatase 2. *J Immunol* **183**:856-864.

Wang H, Brown J and Martin M (2011) Glycogen synthase kinase 3: a point of convergence for the host inflammatory response. *Cytokine* **53**:130-140.

Yao Y, Richman L, Morehouse C, de los Reyes M, Higgs BW, Boutrin A, White B, Coyle A, Krueger J, Kiener PA and Jallal B (2008) Type I interferon: potential therapeutic target for psoriasis? *PLoS One* **3**:e2737.

Zaba LC, Fuentes-Duculan J, Eungdamrong NJ, Abello MV, Novitskaya I, Pierson KC, Gonzalez J, Krueger JG and Lowes MA (2009) Psoriasis is characterized by accumulation of immunostimulatory and Th1/Th17 cell-polarizing myeloid dendritic cells. *J Invest Dermatol* **129**:79-88.

Zheng Y, Danilenko DM, Valdez P, Kasman I, Eastham-Anderson J, Wu J and Ouyang W (2007) Interleukin-22, a T(H)17 cytokine, mediates IL-23-induced dermal inflammation and acanthosis. *Nature* **445**:648-651.

Footnotes

This work was supported by the National Science Council, Taiwan [Grants NSC 96-2320-B-006-018-MY3 and NSC 99-2320-B-006-004-MY3].

Chiou-Feng Lin, PhD.

Institute of Clinical Medicine

College of Medicine

National Cheng Kung University

Tainan 701, Taiwan

886-6-2353535 ext. 4240

886-6-2758781 (fax)

Email: cflin@mail.ncku.edu.tw

JPET Fast Forward. Published on July 6, 2012 as DOI: 10.1124/jpet.112.194100
This article has not been copyedited and formatted. The final version may differ from this version.

Legends for Figures

Fig. 1. IFNGR1 deficiency attenuates TPA-induced acute skin inflammation, including edema, granulocyte infiltration, and CD54 expression but not T cell infiltration. Wild type and IFNGR1-deficient (*Ifngr1*$^{-/-}$) C57BL/6 mice were euthanized 8 h after each ear was individually soaked with PBS, DMSO (solvent control), or TPA (3 μg per ear). Ear tissues were harvested and tissue slices were processed for formalin-fixed paraffin embedding. A, Tissue biopsies (n = 3 per group) were collected for AEC-based immunohistochemistry of phospho-STAT1 Tyr701 (pSTAT1) and STAT1. The histological morphology of the ear biopsies was evaluated from H&E-stained sections (B), and ear thickness (shown in μm) was measured (C). CD45 immunostaining of leukocytes (D), T cells using anti-CD3 (E), granulocytes using anti-Gr-1 (F), and CD54-expressing cells (G) was quantified individually as described in the Materials and Methods. Data measured from the captured fields are shown as the mean ± S.D. from three individual experiments. A representative data set obtained from repeated experiments is shown. ***$p < 0.001$ compared with the DMSO-treated group; #$p < 0.05$; ##$p < 0.01$ compared with wild type. ns, not significant.

Fig. 2. TPA induces GSK-3 activation followed by GSK-3-regulation of IFN-γ signaling. A, AEC-based immunohistochemistry of phospho-GSK-3β Tyr216 (pGSK-3) and phospho-GS Ser431 (pGS) of the ears of wild type C57BL/6 mice (n = 3 per group) individually soaked for 1 h with PBS, DMSO (solvent control), or TPA (3 μg per ear) for 8 h. Representative images from repeated experiments are shown. The expression of total GSK-3β (B), epidermal GSK-3β (C), and dermal GSK-3β (D) was measured from captured fields. Data are shown as the mean ± S.D. of three individual experiments compared with the normalized untreated group (PBS only). *$p < 0.05$ compared with the DMSO-treated group. E, AEC-based immunohistochemistry of phospho-STAT1 Tyr701 (pSTAT1) and STAT1 of the ears of wild type C57BL/6 mice (n = 3 per group) individually soaked with PBS, DMSO (solvent control), or TPA (3 μg per ear) with or without GSK-3 inhibitor BIO (1.5 μg per ear) for 8 h. A representative data set obtained from repeated experiments is shown. F, GSK-3α/β was silenced in HaCaT human keratinocytes using lentiviral-based short hairpin RNA transfection (*shGSK-3α/β* clones 1 and 2). An shRNA targeting luciferase (*shLuc*) was used as a negative control. Western blotting was used to detect the expression of GSK-3α/β. β-actin was used as an internal control. A representative data set obtained from repeated experiments is shown. G The cells were then treated with IFN-γ (10 ng ml^{-1}) or PBS. A luciferase reporter assay of promoter transactivation was used to detect the ratio of IRF1 to Renilla in cells treated with

JPET Fast Forward. Published on July 6, 2012 as DOI: 10.1124/jpet.112.194100
This article has not been copyedited and formatted. The final version may differ from this version.

IFN-γ for 6 h. Data are represented as the mean ± S.D. of triplicate cultures. ***$p < 0.001$ compared with PBS; #$p < 0.05$ compared with IFN-γ. Cells treated with BIO (2.5 μM) were used as a positive control.

Fig. 3. Inhibiting GSK-3 decreases TPA-induced acute skin inflammation but not T cell infiltration. A, H&E staining was used to determine the ear thickness (shown in μm) in wild type C57BL/6 mice ($n = 3$ per group) individually soaked with PBS, DMSO (solvent control), or TPA (3 μg per ear) with or without BIO (1.5 μg per ear) for the indicated time. At 8 h post-treatment, the thickness of ear sections (B) was determined from H&E-stained sections, and immunostaining for leukocytes using anti-CD45 (C), T cells using anti-CD3 (D), granulocytes using anti-Gr-1 (E), and CD54-expressing cells (F) was conducted. Data are shown as the mean ± S.D. of three individual experiments. **$p < 0.01$; ***$p < 0.001$ compared with the DMSO-treated group; #$p < 0.05$; ##$p < 0.01$ compared with the TPA-treated group. ns, not significant.

Fig. 4. Local knockdown of GSK-3 attenuates TPA-induced edema and granulocyte infiltration. Lentiviral-based shRNA (1.2×10^6 p.f.u. of lentivirus per ear) was used to knock down epidermal GSK-3β *in vivo* in the ears of wild type C57BL/6 mice, as described in Materials and Methods. A shRNA targeting luciferase (*shLuc*) was used as a negative control. After 24 h, mouse ears were soaked for 1 h with DMSO (solvent control) and TPA (3 μg per ear). A, AEC-based immunohistochemistry of GSK-3β was performed on the ear tissue of treated mice. B, The expression of GSK-3β was measured from captured fields. Data are shown as the mean ± S.D. of three individual experiments. ##$p < 0.01$ compared with the shLuc group. Ear sections were then examined for H&E staining (C), the ear thickness (D), and immunostaining of granulocytes using anti-Gr-1 (E). Data are shown as the mean ± S.D. of three individual experiments. A representative data set obtained from repeated experiments is shown. ***$p < 0.001$ compared with the DMSO-treated group; #$p < 0.05$; ##$p < 0.01$ compared with the shLuc group.

Fig. 5. Inhibiting GSK-3 decreases TPA-induced IFN-γ production and T-bet nuclear translocation. Wild type C57BL/6 mice ($n = 3$ per group) were euthanized after each ear was individually soaked with PBS, DMSO (solvent control), or TPA (3 μg per ear) with or without BIO (1.5 μg per ear). AEC-based immunohistochemistry was used to determine the expression of IFN-γ at 4 h or 8 h post-treatment (A) and the expression of dermal IFN-γ was measured from captured fields at the indicated time point (B). Data shown are of the mean ±

S.D. of three individual experiments. A representative data set obtained from repeated experiments is shown. ***$p < 0.001$ compared with the DMSO-treated group; #$p < 0.05$ compared with the TPA-treated group. Immunostaining followed by analysis of a single scan of the tissue using a linear sequential confocal laser scanning microscope was used to detect phospho-GSK-3β Y216 (pGSK-3) (C) and the nuclear translocation of T-bet (D) in CD3-positive T cells. DAPI was used for nuclear staining. A representative image from one of the five mice is shown.

Fig. 6. Inhibiting GSK-3 attenuates chronic TPA-induced psoriasis-like skin inflammation including edema, epidermal proliferation, and angiogenesis. A, The time-line of BIO (1.5 μg per ear) treatment for TPA (3 μg per ear)-induced chronic skin inflammation in wild type C57BL/6 mice ($n = 3$ per group). B, H&E stained ear tissue sections ($n = 3$) were examined using a 10× or 20× objective. Image measurement of ear thickness (C), the epidermal thickness (D), and immunostaining of proliferating cells using anti-Ki-67 (E) and endothelial cells using anti-CD31 (F) are shown. Data are shown as the mean ± S.D. of three individual experiments. A representative data set obtained from repeated experiments is shown. ***$p <$ 0.001 compared with the DMSO (solvent control)-treated group; #$p < 0.05$; ##$p < 0.01$ compared with the TPA-treated group. G Representation of the immunohistochemical staining of phospho-GSK-3β Y216 (pGSK-3). A representative data set obtained from repeated experiments is shown.

Fig. 7. Schematic model of GSK-3-facilitated TPA-induced skin inflammation. Following TPA challenge, GSK-3 is initially activated in T cells, followed by keratinocytes. IFN-γ is produced in CD3 T cells in a GSK-3/T-bet-regulated manner. Furthermore, GSK-3 mediates the TPA-induced IFN-γ/STAT1 signaling in keratinocytes and facilitates IFN-γ-induced skin inflammation including edema, immune cell infiltration, and CD54 expression. However, TPA-induced T cell infiltration is independent of IFN-γ and GSK-3. In addition, the mechanism underlying both TPA-mediated activation of GSK-3 and the GSK-3-facilitated IFN-γ-regulated angiogenesis requires further investigation. These findings demonstrate a pathogenic role for GSK-3 in TPA-induced skin inflammation by facilitating IFN-γ expression and signal transduction.

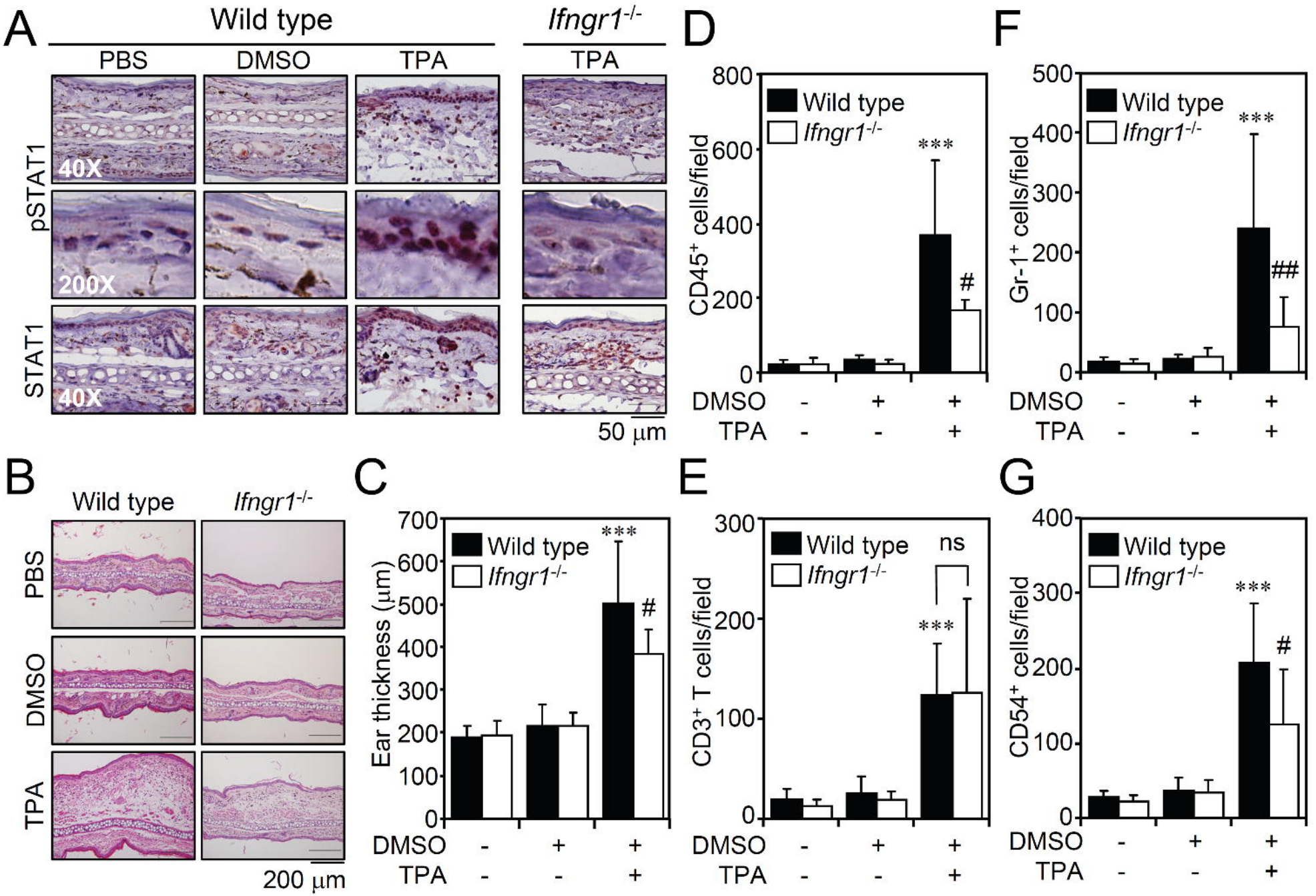
A
Wild type
Ifngr1-/-
PBS
DMSO
TPA
TPA
pSTAT1
STAT1
40X
200X
40X
50 μm
B
Wild type
Ifngr1-/-
PBS
DMSO
TPA
200 μm
C
Ear thickness (μm)
Wild type
Ifngr1-/-
***
#
DMSO - + +
TPA - - +
D
CD45+ cells/field
Wild type
Ifngr1-/-
***
#
DMSO - + +
TPA - - +
E
CD3+ T cells/field
Wild type
Ifngr1-/-
ns
***
DMSO - + +
TPA - - +
F
Gr-1+ cells/field
Wild type
Ifngr1-/-
***
##
DMSO - + +
TPA - - +
G
CD54+ cells/field
Wild type
Ifngr1-/-
***
#
DMSO - + +
TPA - - +

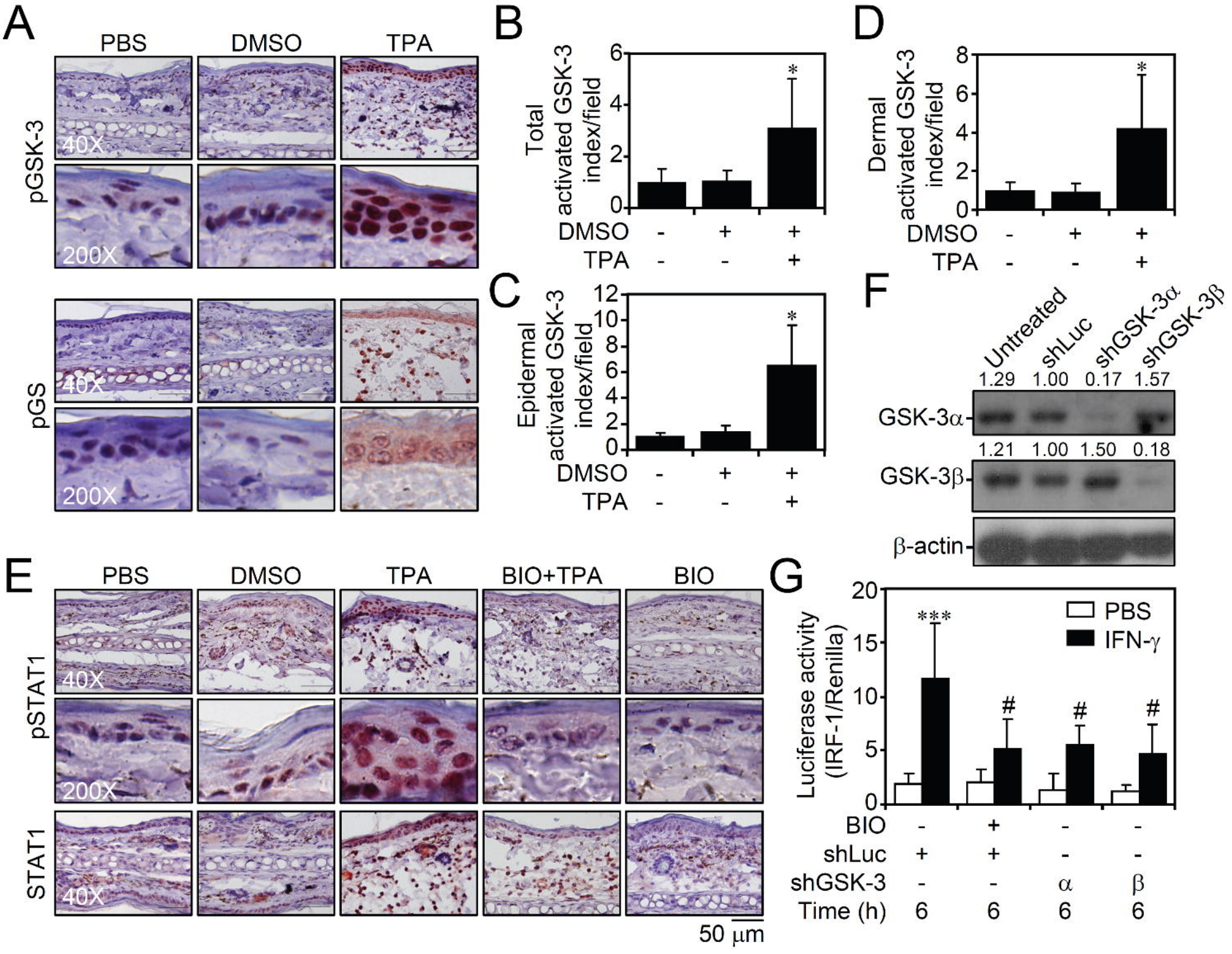
A
PBS
DMSO
TPA
pGSK-3
pGS
40X
200X
B
Total activated GSK-3 index/field
DMSO
TPA
C
Epidermal activated GSK-3 index/field
D
Dermal activated GSK-3 index/field
F
Untreated
shLuc
shGSK-3α
shGSK-3β
1.29 1.00 0.17 1.57
GSK-3α
1.21 1.00 1.50 0.18
GSK-3β
β-actin
E
PBS
DMSO
TPA
BIO+TPA
BIO
pSTAT1
STAT1
50 μm
G
Luciferase activity (IRF-1/Renilla)
PBS
IFN-γ
BIO
shLuc
shGSK-3
Time (h)

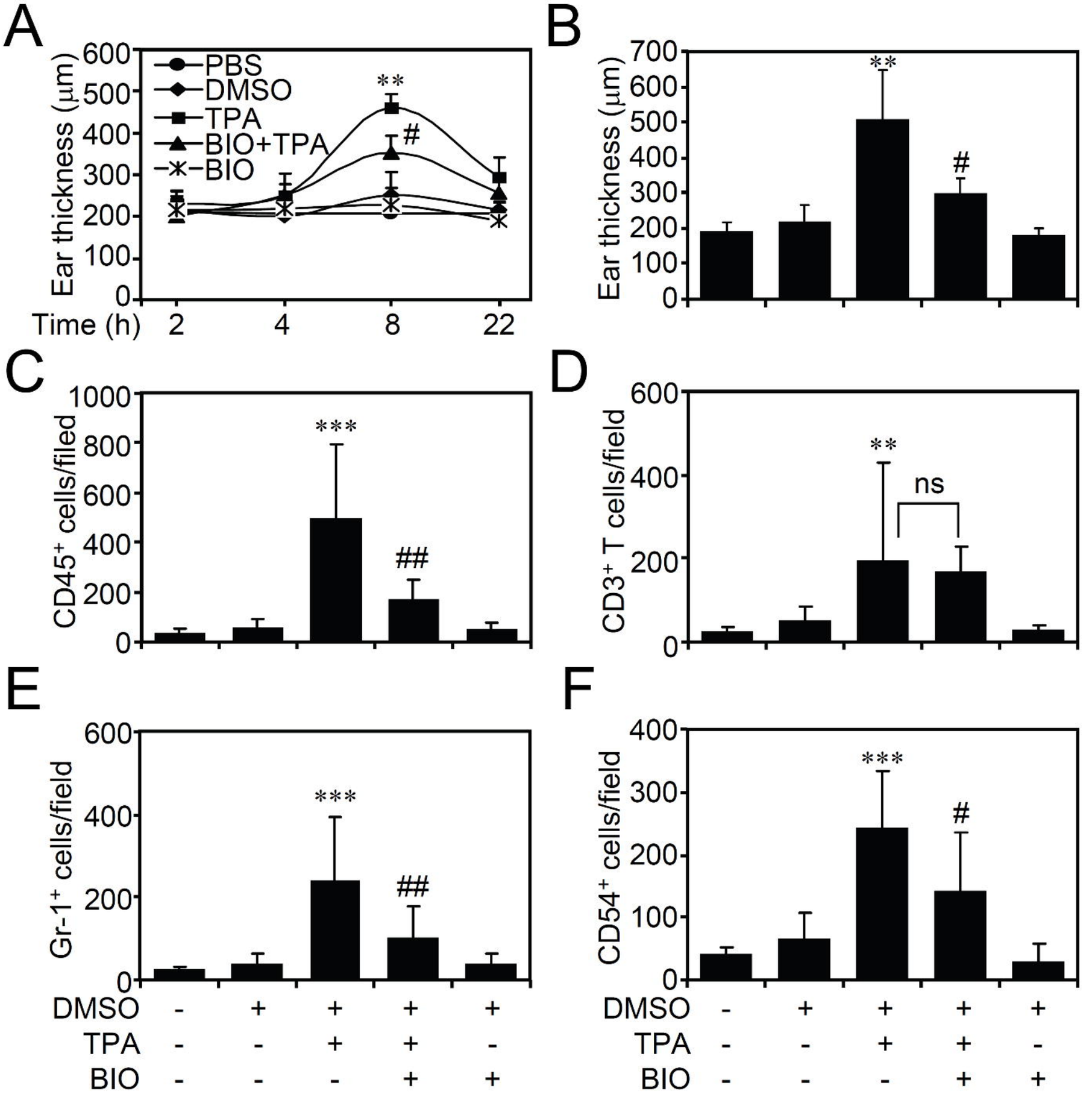
A
Ear thickness (μm)
PBS
DMSO
TPA
BIO+TPA
BIO
Time (h)
2
4
8
22
**
#
B
Ear thickness (μm)
**
#
C
CD45+ cells/filed
***
##
D
CD3+ T cells/field
**
ns
E
Gr-1+ cells/field
***
##
F
CD54+ cells/field
***
#
DMSO
TPA
BIO

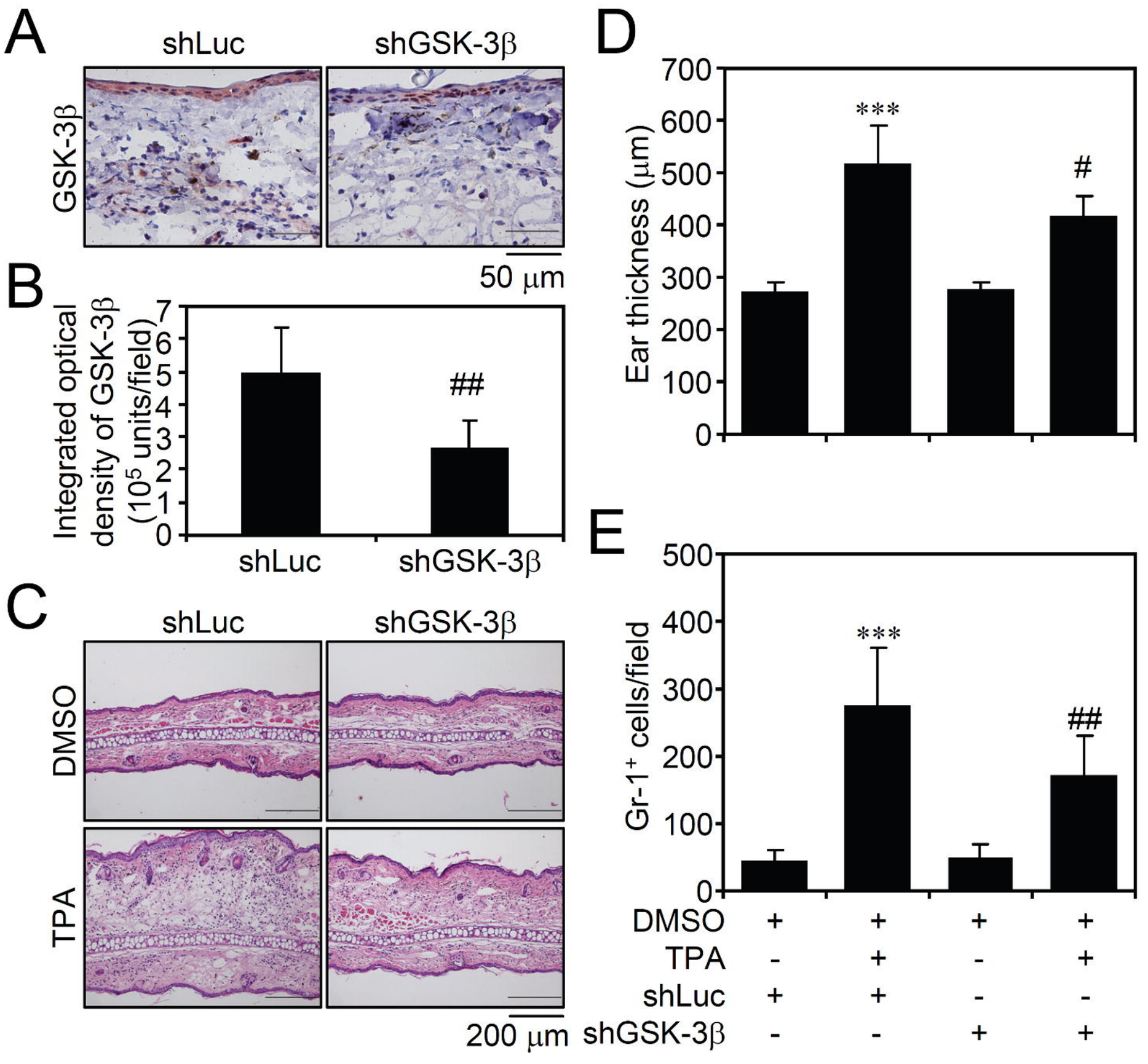
A
shLuc
shGSK-3β
GSK-3β
50 μm
B
Integrated optical density of GSK-3β (10^5 units/field)
0
1
2
3
4
5
6
7
##
shLuc
shGSK-3β
C
shLuc
shGSK-3β
DMSO
TPA
200 μm
D
Ear thickness (μm)
0
100
200
300
400
500
600
700
***
#
E
Gr-1+ cells/field
0
100
200
300
400
500
***
##
DMSO + + + +
TPA - + - +
shLuc + + - -
shGSK-3β - - + +

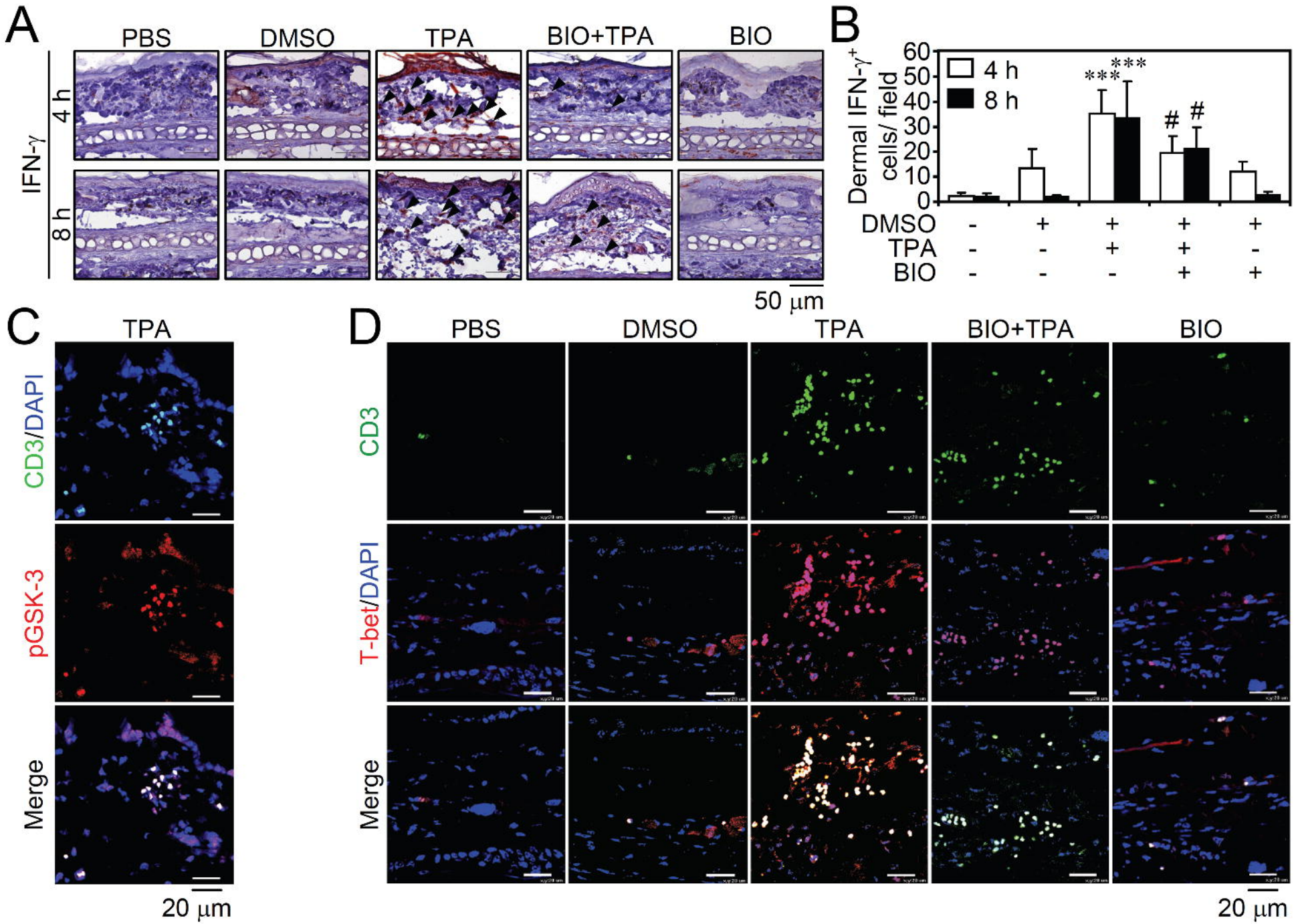
A
PBS
DMSO
TPA
BIO+TPA
BIO
IFN-γ
4 h
8 h
50 μm
B
Dermal IFN-γ+ cells/ field
4 h
8 h
***
***
#
#
DMSO
TPA
BIO
C
TPA
CD3/DAPI
pGSK-3
Merge
20 μm
D
PBS
DMSO
TPA
BIO+TPA
BIO
CD3
T-bet/DAPI
Merge
20 μm

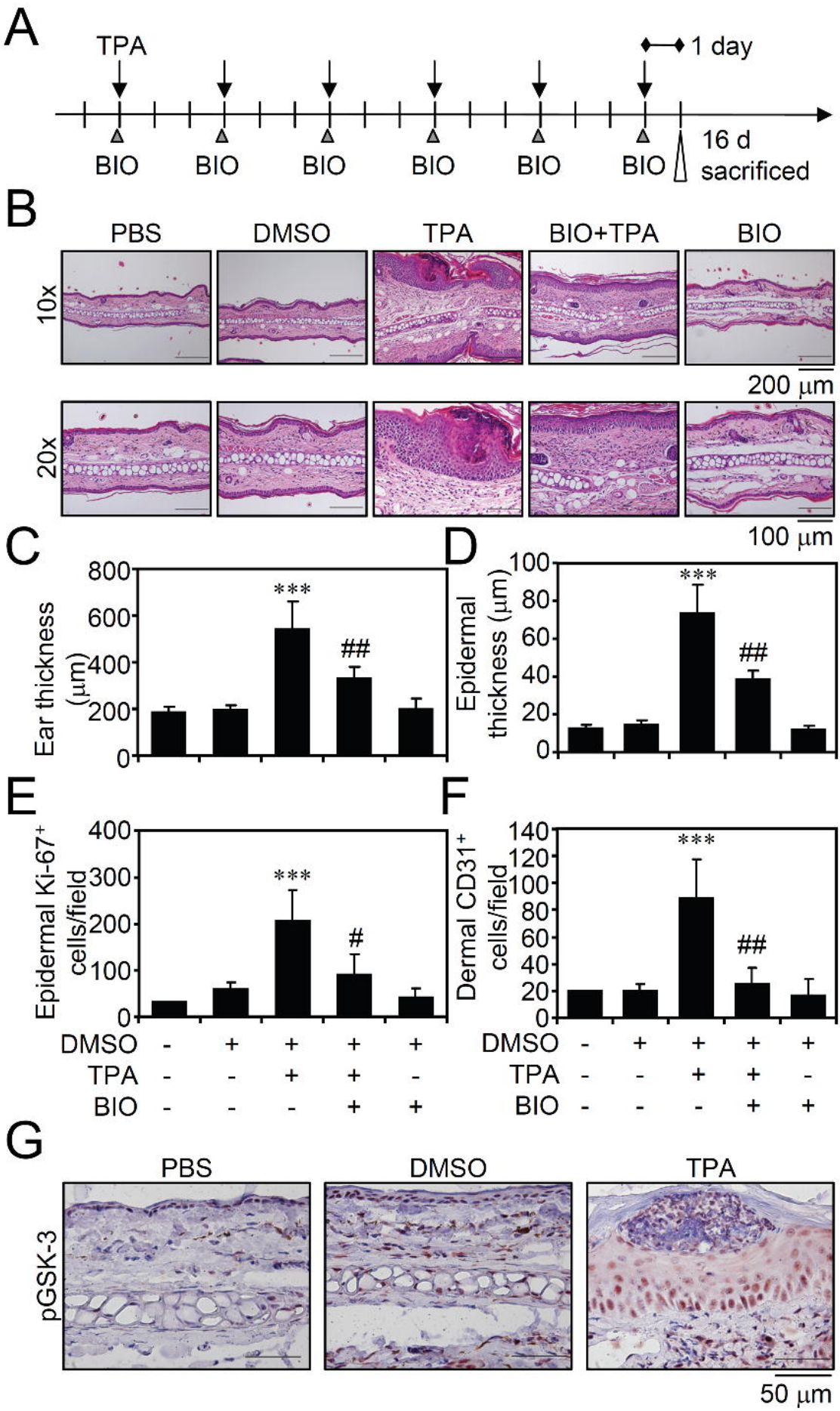
A
TPA
1 day
BIO
BIO
BIO
BIO
BIO
BIO
16 d
sacrificed
B
PBS
DMSO
TPA
BIO+TPA
BIO
10x
200 μm
20x
100 μm
C
Ear thickness (μm)
800
600
400
200
0
***
##
D
Epidermal thickness (μm)
100
80
60
40
20
0
***
##
E
Epidermal Ki-67+ cells/field
400
300
200
100
0
***
#
F
Dermal CD31+ cells/field
140
120
100
80
60
40
20
0
***
##
DMSO - + + + +
TPA - - + + -
BIO - - - + +
G
PBS
DMSO
TPA
pGSK-3
50 μm

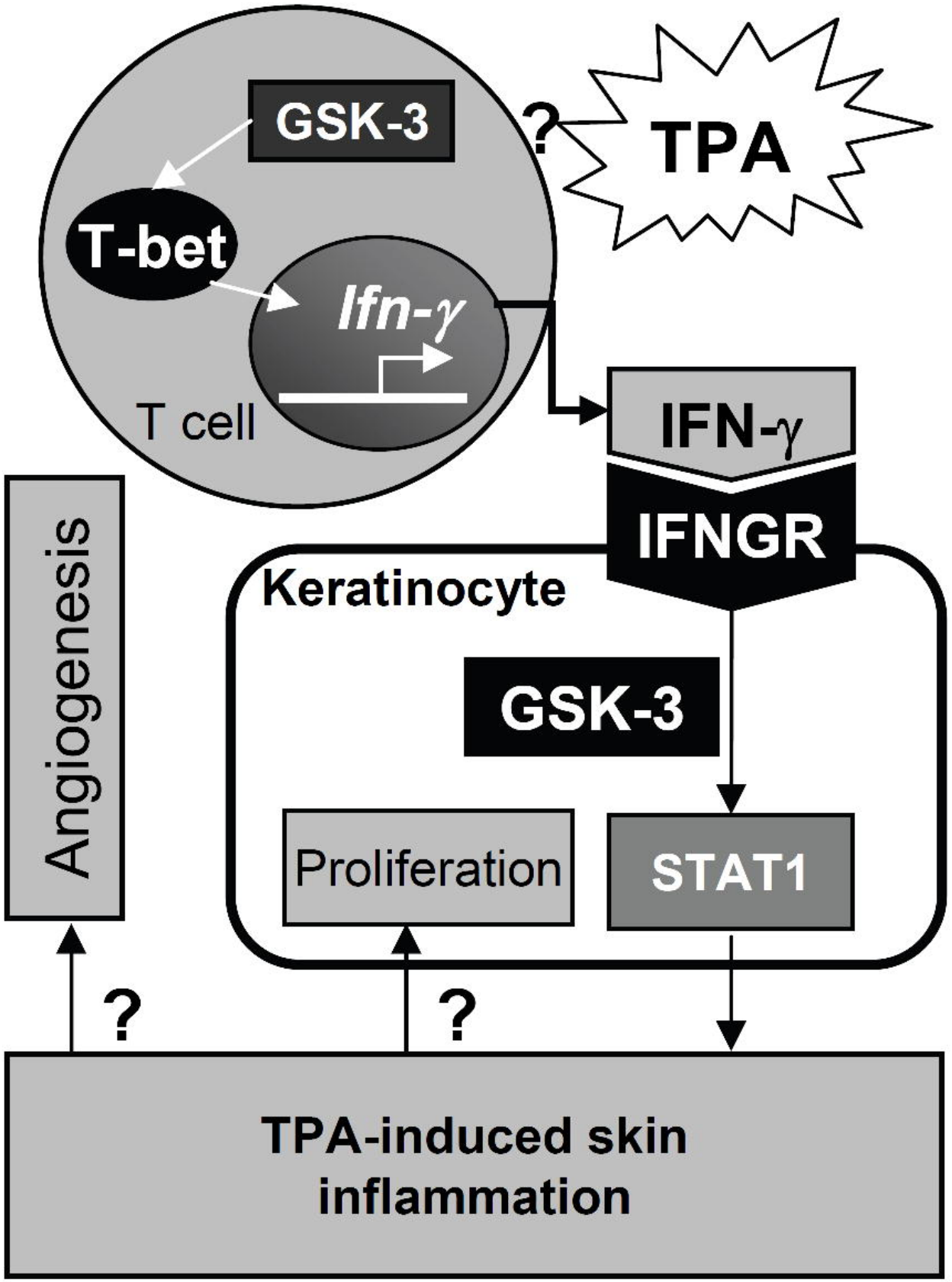
GSK-3
?
TPA
T-bet
Ifn-γ
T cell
IFN-γ
IFNGR
Keratinocyte
GSK-3
Angiogenesis
Proliferation
STAT1
?
?
TPA-induced skin inflammation

Inhibiting Glycogen Synthase Kinase-3 Decreases 12-O-Tetradecanoylphorbol-13-Acetate-Induced Interferon-γ-Mediated Skin Inflammation

Chia-Yuan Hsieh, Chia-Ling Chen, Cheng-Chieh Tsai, Wei-Ching Huang, Po-Chun Tseng, Yee-Shin Lin, Shun-Hua Chen, Tak-Wah Wong, Pui-Ching Choi, and Chiou-Feng Lin

Legends for Supplemental Figures

Fig. S1. Either inhibiting GSK-3 or depleting granulocytes attenuates TPA-induced ear edema. A, Wild type C57BL/6 mice (n = 3 per group) were sacrificed 8 h after each ear was individually soaked for 1 h with PBS, DMSO (in PBS as solvent control), and TPA (3 μg per ear) with or without BIO (1.5 μg per ear). Ear tissue sections (n = 3) were examined for H&E staining with a 10× or 20× objective. A representative data set obtained from repeated experiments is shown. H&E staining with a 10× or 40× objective (B) and images of the measurement of ear thickness (C) were assessed for the effects of granulocyte depletion using anti-Gr-1 depleting antibody in wild type C57BL/6 mice (n = 3) treated with TPA (3 μg per ear). Data are shown as means ± S.D. from three individual experiments. A representative data set obtained from repeated experiments is shown. #$p < 0.05$ compared with TPA treatment alone.

Fig. S2. The GSK-3 inhibitor BIO (1.5 μg per ear) decreases TPA-induced nuclear translocation of T-bet in $CD3^+$ T cells. Immunostaining of T-bet and CD3, shown in three dimensional linear sequential confocal laser screening microscopic observations, was used to study the effect of GSK-3 on TPA-induced T-bet nuclear translocation. DAPI was used for the nuclear staining. Arrowheads indicate T-bet and CD3 double positive T cells. Representative images from repeated experiments are shown.

Fig. S3. Inhibiting GSK-3 decreases TPA-induced epidermal proliferation and angiogenesis. In the model of TPA (3 μg per ear each time)-induced chronic skin inflammation in wild type C57BL/6 mice with or without BIO (1.5 μg per ear each time) (n = 3 per group), immunostaining was used to determine the presence of proliferating cells with Ki-67 and endothelial cells with CD31. DAPI was used for the nuclear staining. A representative data set obtained from repeated experiments is shown.

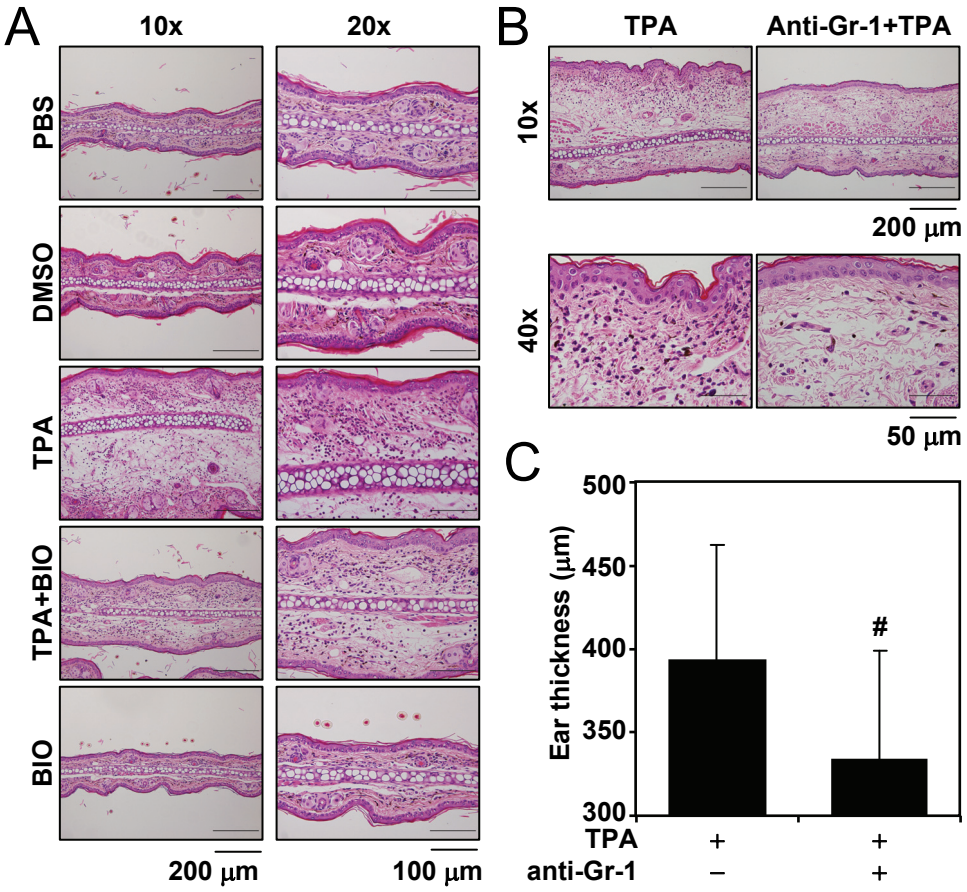

Supplemental Figure 1

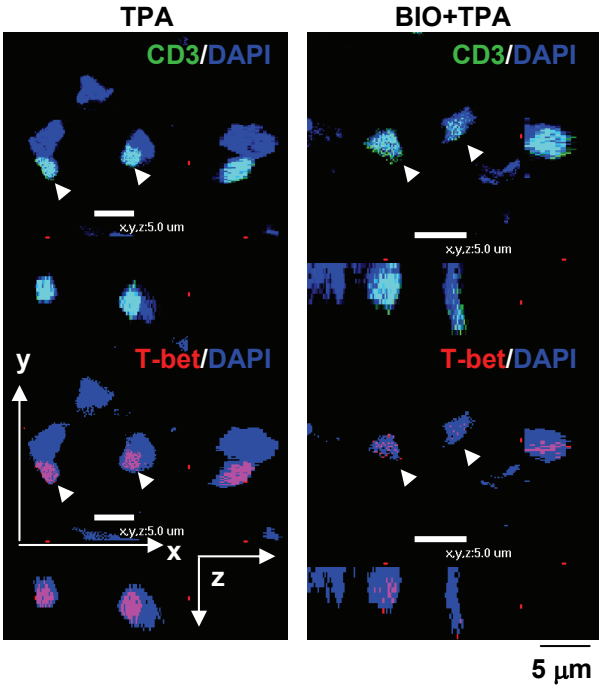

Supplemental Figure 2

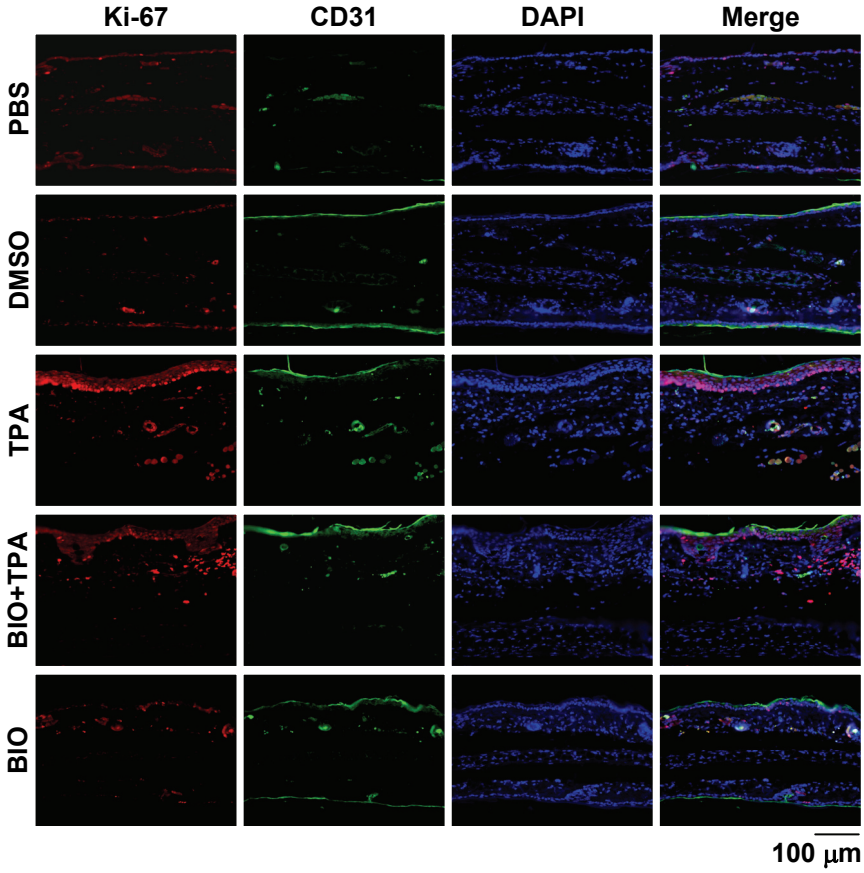

Supplemental Figure 3